Experimental Aortic Intimal Thickening

II. Endothelialization and Permeability

W. S. Webster, DVM, PhD, S. P. Bishop, DVM, PhD and
J. C. Geer, MD

Experimental aortic intimal thickening has been induced in rabbits by two types of injury, suture placement and electrocautery. Scanning electron microscopy showed that endothelialization of the suture plaque was completed at about 10 days following injury. New endothelial cells had no particular orientation or were oriented at right angles to the adjacent normal aortic endothelium. Realignment parallel with the aortic axis had occurred by 21 days after induction of the lesion. Orientation patterns of new endothelial cells over irregularly shaped cautery-induced intimal thickening were difficult to ascertain. Aortic permeability studies were accomplished by using the tracers horseradish peroxidase (HRP) and ferritin. Several naturally occurring intimal thickenings in normal aortas had greater permeability for HRP than did adjacent normal intima. An enhanced penetration of both tracers was observed in mature intimal lesions produced by both experimental procedures compared to adjacent morphologically normal aortic intima. HRP molecules entered the thickened aortic intima in increased amounts through interendothelial junctions and by endothelial pinocytotic vesicles; ferritin molecules were seen only in pinocytotic vesicles. Increased penetration of HRP was observed for as long as 27 weeks after injury, while that of ferritin was observed only for 3 weeks. The enhanced permeability of the thickened intima as compared to normal for these two tracers of considerably different sizes strongly suggests an increased permeability of endothelium overlying intimal thickening for naturally circulating macromolecules (Am J Pathol 76:265–284, 1974).

FOCAL ARTERIAL INTIMAL THICKENING commences in infancy and gradually increases with age.[1,2] Anatomic sites of intimal thickening in man have been found to correspond rather closely to those sites at which atherosclerotic plaques are prone to develop.[3] Numerous authors have proposed that this fibromuscular intimal thickening predisposes to development of the lipid-laden atherosclerotic plaque in man [4–7] and in experimental animals.[8–11]

If fibrous intimal thickening does have a predisposition to deposition of blood macromolecules, morphologic and permeability abnormalities

From the Department of Veterinary Pathobiology, College of Veterinary Medicine and the Department of Pathology, College of Medicine, The Ohio State University, Columbus, Ohio.

Supported in part by Grant HL-11897 from the US Public Health Service, a grant from Harker's Fund and a College of Medicine General Research Support Grant.

Accepted for publication April 25, 1974.

Address reprint requests to Dr. Jack C. Geer, Office of Pathology, 4170 Graves Hall, 333 W Tenth Ave, Columbus, OH 43210.

may be demonstrable in the endothelium. Structural alteration of the arterial surface may be associated with increased permeability for various substances in experimentally injured arteries.[12,13] Evidence from scanning microscopic studies [14] and *en face* studies [15] indicates that new endothelium located over induced aortic lesions in rabbits is morphologically abnormal. Demonstration of enhanced permeability with tracers in healed experimental intimal thickening would lend support to the contention that blood-borne substances may more readily enter the thickened than nonthickened intima.

The purpose of this investigation was to study the process of endothelialization of newly forming intimal plaques in injured rabbit aortas by scanning microscopy, and to determine permeability characteristics of the lesion surface using electron microscopic tracer technics.

Materials and Methods

The methods for producing aortic intimal thickening by suture placement and electrocautery in young rabbits have been reported.[16] Briefly, using aseptic surgical technic, a 4-0 silk suture was placed in the thoracic aorta at T_6, and an electrocautery lesion, 0.5 cm in diameter, was produced on the adventitial surface of the aorta at T_4 and T_8.

Scanning Electron Microscopy

Seventeen animals were killed, by glutaraldehyde perfusion, sequentially from 2 to 49 days after surgery as previously described.[16] All experimentally produced aortic lesions and control aortas were sectioned transversely and tissues for scanning electron microscopy were fixed for 1.5 hours in 2% glutaraldehyde and stored in phosphate buffer, pH 7.35, at 4 C. Tissues were successively dehydrated in ascending concentrations of ethyl alcohol, two changes of each being made every 10 minutes. Tissue was processed by critical point drying, according to Anderson [17] with amyl acetate as the intermediate fluid, and carbon dioxide as the transitional fluid. Dried tissue was mounted on graphite in alcohol (Dag 154, Acheson Colloids Company, Port Huron, Michigan) on an aluminum stub and coated with 200- to 300-Å layer of gold, using a rotating stage evaporator (Denton DV502, Denton Vacuum, Inc, Cherry Hill Industrial Center, Cherry Hill, NJ). Specimens were examined with a Cambridge Stereoscan Mark II A microscope, at magnifications of 100 to 10,000. One to three sections of both suture- and cautery-induced lesions from each time interval were examined.

Permeability

Rabbits from postoperative periods 3, 5, 7, 14, 21 and 27 weeks were given an intravenous injection of horseradish peroxidase (HRP) (Sigma Chemical Company, Type II, RZ 1.9) at a dose of 8 mg/100 g body weight in 0.5 ml physiologic saline/100 g body weight. Animals were killed at 2 or 20 minutes after administration of the tracer. Tissue sections from animals receiving horseradish peroxidase were incubated for 1 hour in the Graham-Karnovsky medium [18] (10 mg 3,3'diaminobenzidine tetrahydrochloride, 10 ml 0.05 M Tris HCl buffer, pH 7.6, containing 0.01% hydrogen peroxide) prior to postfixation in osmium tetroxide to obtain

peroxidase reaction product. Postfixed tissues were processed for electron microscopy, and unstained tissue sections were examined as previously described.[16]

Ferritin (Ferritin, horse spleen, twice crystallized, Nutritional Biochemical Corp, Cleveland, Ohio) was used to assess endothelial permeability at periods 3 through 7 weeks after surgery. Prior to sacrifice, rabbits were given a single intravenous injection of ferritin preparation, at a dose of 1 mg/g body weight. Ferritin was prepared by removing excess cadmium from commercial ferritin solution by dialysis according to the method of Farquhar.[19] The solution was then concentrated by sedimentation at 105,000g for 10 hours in a preparative ultracentrifuge (L-2 Ultracentrifuge, Beckman Instruments, Inc, Fullerton, Calif) and resuspended to volume in saline. Infused animals were killed, in the same manner as those receiving HRP, 2 or 30 minutes after ferritin injection. Tissues from experimental lesions and control aorta were processed (without incubation) and examined, as were the HRP-treated tissues in a Hitachi Perkin-Elmer electron microscope HU 11 B2 at 50 kV.

Results

Endothelialization

Sequential changes in the surface of the thickening intima are reported separately for the suture- and cautery-induced lesions, as there were distinct differences in the appearance of the lesions. When compared to the normal aorta, intimal lesions induced by either means have demonstrable surface alterations. The surface of the perfused, normal aorta usually appeared as a series of parallel troughs and disrupted ridges (endothelial nuclei), which were oriented parallel with the aortic axis (Figure 1). In some samples, apparently because of more effective perfusion, the luminal surface was relatively flat and endothelial ridges were barely detectable.

The surface of suture-induced lesions had a consistent sequence of morphologic changes. Moderate numbers of leukocytes, erythrocytes and platelets were attached to suture fibers in the 2- to 5-day-old lesions (Figures 2 and 3). Occasional blood monocytes were observed attached to the silk fibers by long cytoplasmic processes. Small amounts of fibrin were deposited on the suture in early lesions.

Endothelialization was observed in various stages of progression over all suture lesions. The earliest lesions (2 to 3 days) had few if any endothelial cells adhered to the suture mass. New endothelium was present at the base and on the sides of the suture at 5 days (Figure 4). The border of the growing sheet of endothelium was generally uneven. Newly formed endothelium appeared remarkably free of attached blood cells, in contrast to the adjacent exposed silk fibers. By 7 days, in some lesions the entire suture was covered by endothelium. All lesions at 10 days were completely endothelialized (Figure 5).

Differences in endothelial cell orientation were observed as the suture-induced intimal thickening matured. At 10 days after injury, new endothelial cells near the base of the suture were oriented parallel with the aortic axis, while those cells on the upper sides and top of the suture were either circularly arranged or had no particular orientation (Figures 5 and 6). After 21 days, most new endothelial cells, regardless of their location, were oriented longitudinally (parallel with the aortic axis) (Figure 7). This orientation is similar to that of normal aortic endothelium.

Reendothelialization of the intimal surfaces of cauterized aortas was also visualized with scanning microscopy. Focal, random loss of endothelial cells was apparent in early lesions; remaining endothelial cells in the center and at the periphery of deendothelialized areas appeared distorted. Flat granular areas of the lesion were studded with numerous leukocytes, erythrocytes and platelets at 2 through 7 days. Strands or clumps of fibrin were seen on denuded aortic surfaces through the first week. By 7 to 10 days, however, the surface was covered with new endothelium which had few attached blood cells and little fibrin.

The reorientation of new endothelial cells observed in suture-induced lesions was not so obvious in cautery lesions. Aortic surface elevation of cautery-induced intimal thickening was first recognized by scanning microscopy at about 10 days. These elevations were variously shaped, from flattened mounds to sloping hillocks to long thin elevated ridges. Endothelial cells on the sides of the intimal mounds were oriented parallel with the aortic axis and normal aortic endothelium. The surface of intimal mound plateaus was decidedly more flat than that of the sides or of normal aortic surface (Figure 8); nuclei of plateau endothelial cells were noticably round and flat, and had no particular alignment when compared to adjacent normal endothelial cell nuclei. Endothelial cell patterns in lesions three or more weeks after cauterization generally suggested a longitudinal orientation of cells; however, lesions with all endothelial cells aligned parallel with the aortic axis were not observed at any time after injury.

Permeability

Hemodynamic changes occurred in several monitored rabbits after ferritin but not horseradish peroxidase infusion. Aortic blood pressure was temporarily decreased in one animal to approximately 60/40 (systolic/diastolic) mmHg during ferritin infusion but returned to normal levels (120/80 mmHg) by about 5 minutes after infusion. Another rabbit showed a slight transient decrease in heart rate and a slight de-

crease in aortic pulse pressure. Horseradish peroxidase infusion had no apparent effect on heart rate or systemic blood pressure.

Permeability differences for horseradish peroxidase and ferritin were observed in the normal rabbit aorta. The flocculent electron-dense horseradish peroxidase reaction product was found in the interendothelial spaces of normal aorta and within endothelial plasmalemmal vesicles, irregardless of time after injection of peroxidase. Ferritin localization in nomal aorta differed from that of peroxidase in that the electron-dense ferritin molecules were found only within endothelial plasmalemmal vesicles and microvesicular bodies (Figure 12). Ferritin, in contrast to horseradish peroxidase, was never observed in the interendothelial junctions or the subendothelial space of normal arteries.

Naturally occurring intimal thickenings of one to three cell layers were observed in several control aortas. In these thickenings, peroxidase reaction product was present in greater amount than was observed in adjacent normal intima (Figure 9). Reaction product was seen principally in endothelial cytoplasmic vesicles and interendothelial junctions, but modest amounts were present in the subendothelial space and intimal cell cytoplasmic vesicles. Spontaneous intimal thickenings were not found in rabbits injected with ferritin tracer.

Enhanced permeability of suture and cautery lesions was evidenced by the presence of large amounts of peroxidase reaction product and ferritin in the same transendothelial routes demonstrated for each tracer in the normal aortic endothelium. Permeability patterns for the two tracers are described first for lesions caused by sutures, then for those caused by cautery. The quantity and extent of penetration of horseradish peroxidase molecules in suture-induced intimal thickenings were markedly greater than that observed in normal aorta and were similar at 3 through 27 weeks after suture placement. In some instances, the striking penetration was appreciated by light as well as electron microscopy. Light microscopic examination of toluidine blue–stained aortic sections revealed much greater amounts of the brown-staining enzyme product in the juxtaluminal portions of induced intimal thickening than in the juxtaluminal portions of control aortas. Ultrastructurally, suture lesions typically had reaction product in the interendothelial junctions and in lateral, basal and cytoplasmic endothelial plasmalemmal vesicles (Figure 10). Regardless of the age of the lesion, the greatest amounts of product were nearly always present in the subendothelial space, occurring in a decreasing gradient away from the endothelium (Figure 11). Highest concentrations were found immediately under endothelial cells, and product was still detectable four to five subendothelial cell layers

deep over all regions of intimal thickening. In the tapering margins of the intimal thickening, enzyme was present in the interstitium from the endothelium to the internal elastic lamina. Plasmalemmal vesicles of the more superficially located subendothelial cells were observed to contain reaction product. In general, longer periods for diffusion of peroxidase into suture lesions of the same age resulted in greater quantities of reaction product being found in subendothelial cells and the interstitium.

Although ferritin molecules were much less frequent in tissue sections than was peroxidase product, modest numbers were found in aortas with suture-induced intimal thickening (Figures 13 and 14). Enhanced ferritin passage into the thickened intima was best demonstrated in lesions 3 weeks after injury (Figure 13). Ferritin particles were uniformly scattered throughout the subendothelial space for several cell layers and within microvesicular bodies of the more superficially located subendothelial cells (Figure 14). As was true for peroxidase localization in lesions of all ages, endothelial cells had relatively greater numbers of vesicles with ferritin molecules than did adjacent subendothelial cells. An increase in numbers of ferritin molecules in induced intimal thickenings could not be documented in lesions older than 3 weeks.

Discussion

The circumferential orientation of regenerated endothelial cells in the early suture lesion, at right angles to those in the adjacent normal aorta and to blood flow, was an unexpected finding. Cell orientation over intimal thickening was influenced by time and the topography of the lesion. The circumferential pattern of cells over the suture appeared to be a manifestation of endothelial cell shape during growth or migration over a nonendothelialized area. The cells assumed an elongated shape oriented in the direction of growth during the active growth phase. After growth had ceased, cell orientation appeared to be influenced by hemodynamic or other factors. Cell alignment was then parallel with blood flow, a finding in agreement with aortic resection studies [20] in which endothelial cell axes were shown to turn 90° so that they settled parallel with direction of blood flow. Cautery lesions appeared to endothelialize from all sides simultaneously, with variously shaped cells growing in from the edges of the lesions as well as from remaining islands of viable endothelium. Orientation of endothelial cells over cautery-induced intimal thickening was more difficult to assess due to the irregular shapes and contours of the lesions. Turbulent blood flow, as may have oc-

curred locally over cautery-induced lesions, is capable of disorienting aortic endothelial cells.[20]

We were unable to visualize, by scanning electron microscopy, the reported obliquely oriented "intercellular bridges" occurring between arterial endothelial cells.[21,22] These bridges may have been artifactual, as tissues were obtained from nonperfused animals. Basis for function of the bridges in controlling width of intercellular clefts obviously could not be substantiated in our study.

The relationship of endothelial cell orientation and permeability characteristics of intimal thickenings may be important. As we did not study permeability in relatively early lesions (younger than 3 weeks), we have no information on the influence of reorienting endothelial cells on the passage of circulating tracer molecules into lesions. Future research should be directed towards elucidation of the functional behavior of regenerated endothelium during this early period of cell reorientation.

Increased endothelial permeability for the smaller molecule, peroxidase, persisted for as long as 27 weeks after injury (the maximal time period studied), whereas increased permeability for the larger molecule was evident only at the earliest period studied, 3 weeks. There was no recognizable difference in the magnitude of increased permeability between the suture and cauterization lesions, indicating that the type of injury plays little if any role in determining permeability characteristics of the resulting lesion. The thickness of the intimal lesion likewise did not appear to determine permeability, as no difference was discernable between thick and thin portions of the same lesion or in comparison of thick to thin lesions.

The specific mechanism(s) by which aortic permeability is enhanced was not investigated. The results of our study on peroxidase permeability support the findings of others that this enzyme crosses arterial endothelium by interendothelial clefts [13,23] and by vesicular transport.[23] Macromolecules are generally thought to enter and traverse endothelial cells only by pinocytosis. Isotopic cholesterol flux studies on atherosclerotic lesions of pigeons [9] and kinetic studies of cholesterol uptake by endothelium of the normal rabbit aorta [24] support this contention. Ferritin, with a molecular weight of 500,000, crosses the endothelial barrier solely by vesicular transport.[13,25-27] Increased numbers of pinocytotic vesicles in endothelial cells, as might be expected in our lesions with an increased incorporation of ferritin, were not apparent. However, enhanced endothelial vesicular transport by both tracers was readily demonstrated, suggesting an increased metabolic activity of

these cells. Ultrastructurally, the increased numbers of various cytoplasmic organelles observed in endothelial cells of the intimal lesions tend to support the energy-dependent production of vesicular membranes required for pinocytosis.[16]

The results of this study suggest that endothelial permeability varies with regard to size of the molecules transported and maturity of the endothelial cell. The newly formed endothelial cells show enhanced permeability to both large and small molecules in comparison to endothelium over normal intima. The permeability for the smaller molecule persists for a long period of time, whereas that for the larger molecule is evident only in the newly formed endothelium. Enhanced endothelial permeability for small molecules also was evident in foci of spontaneous intimal thickening. Unfortunately spontaneous intimal thickening was not observed in ferritin experiments to confirm the findings in experimental lesions. The significance of the findings of the present experiment with regard to human arterial intimal thickening and its possible predisposition to atherosclerosis is not evident and can only be a subject for speculation. That foci of experimental intimal thickening are predisposed to lipid accumulation appears well established;[8-11] however, the mechanism by which the lipid accumulates is unknown. To further our understanding of endothelial transport it is necessary that future studies employ a variety of tracers that encompass the variable of not only molecule size but also shape, charge and exchangability of components of a macromolecule with constituents of the endothelial cell (*eg*, cholesterol).

References

1. Daoud A, Jarmolych J, Zumbo A, Fani K, Florentin R: "Preatheroma" phase of coronary atherosclerosis in man. Exp Mol Pathol 3:475–484, 1964
2. Gross L, Epstein, EZ, Kugel MA: Histology of the coronary arteries and their branches in the human heart. Am J Pathol 10:253–274, 1934
3. Sappington SW, Cook HS: Radial artery changes in comparison with those of the coronary and other arteries. Am J Med Sci 192:822–839, 1936
4. Dock W: The predilection of atherosclerosis for the coronary arteries. J Am Med Assoc 131:875–878, 1931
5. Wilens SL: The nature of diffuse intimal thickening of arteries. Am J Pathol 27:825–833, 1951
6. Prior JT, Jones DB: Structural alterations within the aortic intima in infancy and childhood. Am J Pathol 28:937–945, 1952
7. Movat HZ, More RH, Haust MD: The diffuse intimal thickening of the human aorta with aging. Am J Pathol 34:1023–1028, 1958
8. Westlake GE, Grundy SM, O'Neal RM: The effect of an atherogenic diet on pre-existing aortic intimal thickenings in old dogs. Exp Mol Pathol Suppl 1:1–8, 1963

9. Lofland HB, Clarkson TB: The bi-directional transfer of cholesterol in normal aorta, fatty streaks, and atheromatous plaques. Proc Soc Exp Biol Med 133: 1–8, 1970

10. Moss NS, Benditt EP: The ultrastructure of spontaneous and experimentally induced arterial lesions. III. The cholesterol-induced lesions and the effect of a cholesterol and oil diet on the preexisting spontaneous plaque in the chicken aorta. Lab Invest 23:521–535, 1970

11. Hardin NJ, Minick CR, Murphy GE: Experimental induction of atherosclerosis by the synergy of allergic injury to arteries and lipid-rich diet. III. The role of earlier acquired fibromuscular intimal thickening in the pathogenesis of later developing atherosclerosis. Am J Pathol 73:301–326, 1973

12. Duff G, McMillan GC, Lautsch EV: The uptake of colloidal thorium dioxide by the arterial lesions of cholesterol atherosclerosis in the rabbit. Am J Pathol 30:941–955, 1954

13. Hüttner I, More RH, Rona G: Fine structural evidence of specific mechanism for increased endothelial permeability in experimental hypertension. Am J Pathol 61:395–405, 1970

14. Shimamoto T: An introduction to the investigation of atherogenesis, thrombogenesis and pyridinolcarbamate treatment: visualization of the transendothelial passage through intercellular junctions and discovery of endothelial folds and intercellular bridges of vascular endothelium. Excerpta Med Int Congr Ser 201:5–27, 1969

15. Poole JCF, Sanders AG, Florey HW: The regeneration of aortic endothelium. J Pathol Bacteriol 25:133–143, 1958

16. Webster WS, Bishop SP, Geer JC: Experimental aortic intimal thickening. I. Morphology and source of intimal cells. Am J Pathol 76:245–264, 1974

17. Anderson TF: Electron microscopy of microorganisms, Physical Techniques in Biological Research, Vol III, Part A, Cells and Tissues. Edited by AW Pollister. New York, Academic Press, Inc, 1966, pp 336–364

18. Graham RC, Karnovsky MJ: The early stages of absorption of injected horseradish peroxidase in the proximal tubules of mouse kidney: ultrastructural cytochemistry by a new technique. J Histochem Cytochem 14:291–302, 1966

19. Farquhar MG, Palade GE: Glomerular permeability. II. Ferritin transfer across the glomerular capillary wall in nephrotic rats. J Exp Med 114:699–716, 1961

20. Flaherty JT, Pierce JE, Ferrans VJ, Patel DJ, Tucker WK, Fry DL: Endothelial nuclear patterns in the canine arterial tree with particular reference to hemodynamic events. Circ Res 30:23–33, 1972

21. Shimamoto T, Yamashita Y, Sunaga T: Scanning electron microscopic observation of endothelial surface of heart and blood vessels: the discovery of intercellular bridges of vascular endothelium. Proc Jap Acad 45:507–511, 1969

22. Sunaga T, Yamashita Y, Shimamoto T: The intercellular bridge of vascular endothelium: the presence of two types of bridges of endothelial surface. Proc Jap Acad 45:627–631, 1969

23. Anversa P, Giacomelli F, Wiener J, Spiro D: Permeability properties of ventricular endocardium. Lab Invest 28:728–734, 1973

24. Jensen J: The kinetics of the *in vitro* cholesterol uptake at the endothelial cell surface of the rabbit aorta. Biochim Biophys Acta 135:544–556, 1967

25. Hüttner I, Boutet M, More RH: Studies on protein passage through arterial endothelium. II. Regional differences in permeability to fine structural protein tracers in arterial endothelium of normotensive rat. Lab Invest 28:678–685, 1973

26. Bruns RR, Palade GE: Studies in blood capillaries. II. Transport of ferritin molecules across the wall of muscle capillaries. J Cell Biol 37:277–299, 1968

27. Clementi F, Palade GE: Intestinal capillaries. I. Permeability to peroxidase and ferritin. J Cell Biol 41:33–58, 1969

Legends for Figures

Fig 1—Perfused normal rabbit aorta. The aortic longitudinal axis is indicated by the *arrow*. Several erythrocytes (*E*) and an occasional leukocyte (*L*) are present on the endothelium. Longitudinally oriented endothelial nuclei bulge into the lumen (20 kV, × 950).

Fig 2—Lateral view of suture (*S*) resting on luminal surface of aorta (*A*) 2 days after placement. Blood cells and fibrin (*F*) cling to the interwoven silk fibers (5 kV, × 310).

Fig 3—Juncture of suture and aorta (*A*) 2 days after suture placement. Fibrin meshwork (*F*) with numerous erythrocytes covers a portion of the suture. Several endothelial cells (*E*) at the juncture are obliquely separated from the adjacent normal endothelial sheet (5 kV, × 4000).

Fig 4—Juncture of suture and aorta (*A*) 5 days after suture placement. Silk fibers are exposed (*arrow*) or are covered with granular-appearing clumps of fibrin (*F*) and various blood cells. There are prominent intercellular junctions of new endothelial cells (*E*) on the sides of the suture (5 kV, × 720).

Fig 5—Lateral view of completely endothelialized 10-day-old suture plaque. The *arrow* on top of the suture indicates aortic and suture axes. Nuclei of aortic endothelial cells (*A*) adjacent to the suture are spindle shaped and directed parallel with the aortic axis. Nuclei of new endothelial cells (*E*) are ovoid, disc-shaped and show no orientation with regard to the vessel axis (10 kV, × 360).

Fig 6—Oblique view of top of suture shown in Figure 5 illustrating definite circular orientation of endothelium at right angles to the long axis of the suture (5 kV, × 880).

Fig 7—Completely endothelialized 21-day-old suture lesion. Cut end of suture is visible in lower left corner. *Arrows* indicate aortic axis. Endothelial cells (*E*) atop the suture are oriented parallel with the suture and aortic axis (3 kV, × 180). **Inset**—Greater magnification of endothelium on top of suture. Compare cell direction with that in Figs 5 and 6 (3 kV, × 620).

Fig 8—Luminal surface of rabbit aorta 21 days after cautery. *Long arrow* indicates aortic axis. The focal, elevated intimal mound has a flattened plateau. Plateau endothelial cells (*arrows*) are not visible in relief as are those of the adjacent endothelium (*A*) (3 kV, × 790).

Fig 9—"Normal" rabbit aorta 7 weeks after surgery, 20 minutes after peroxidase infusion. Electron-dense reaction product is visible in cytoplasmic vesicles (*open arrows*) of endothelial (*E*) and, to a lesser extent, of the slender subendothelial (*S*) cells. Some product is also present between endothelial cells and in the subendothelial space (*closed arrows*) (Unstained × 14,800).

Fig 10—Intimal thickening of a 7-week-old suture lesion, 20 minutes after horseradish peroxidase infusion. Aortic lumen (*L*) and portions of endothelial cells (*E*). Electron-dense horseradish peroxidase reaction product is present in the space between endothelial cells, the adjacent plasmalemmal vesicles (*closed arrows*), scattered throughout the subendothelial space and in plasmalemmal vesicles (*open arrow*) of subendothelial cells (*S*) (Unstained, × 45,000).

Fig 11—Suture-induced intimal thickening 3 weeks after surgery, 20 minutes after peroxidase infusion. *L*=aortic lumen, *E*=endothelial cells, *S*=subendothelial cells. Most peroxidase reaction product is present in the intercellular spaces of the more superficial intima (*closed arrows*). Product is also visible in cytoplasmic vesicles of both endothelial cells and subendothelial muscle cells (*open arrow*) (Unstained, × 11,200).

Fig 12—"Normal" rabbit aorta 7 weeks after surgery, 30 minutes after ferritin infusion. *L*=aortic lumen, *E*=endothelial cells. Ferritin particles are present within cytoplasmic vesicles (*arrows*) of an endothelial cell, but not between endothelial cells or within the subendothelial space. Only rarely was this quantity of ferritin seen in similarly sized fields of normal aorta (Unstained, × 44,300).

Fig 13—Suture-induced intimal thickening 3 weeks after surgery, 30 minutes after ferritin infusion. *L*=aortic lumen, *E*=endothelial, *S*=subendothelial cells. Electron-dense ferritin molecules are present within microvesicular bodies of endothelial and subendothelial cells (*open arrows*), as well as in the subendothelial space (*closed arrow*) (Unstained, × 65,000).

Fig 14—Suture-induced intimal thickening 3 weeks after surgery, 30 minutes after ferritin infusion. Portion of an endothelial cell (*E*) overlies portions of two subendothelial cells (*S*). Ferritin molecules are seen within cytoplasmic microvascular bodies (*arrows*) of a subendothelial cell (Unstained, × 45,500).

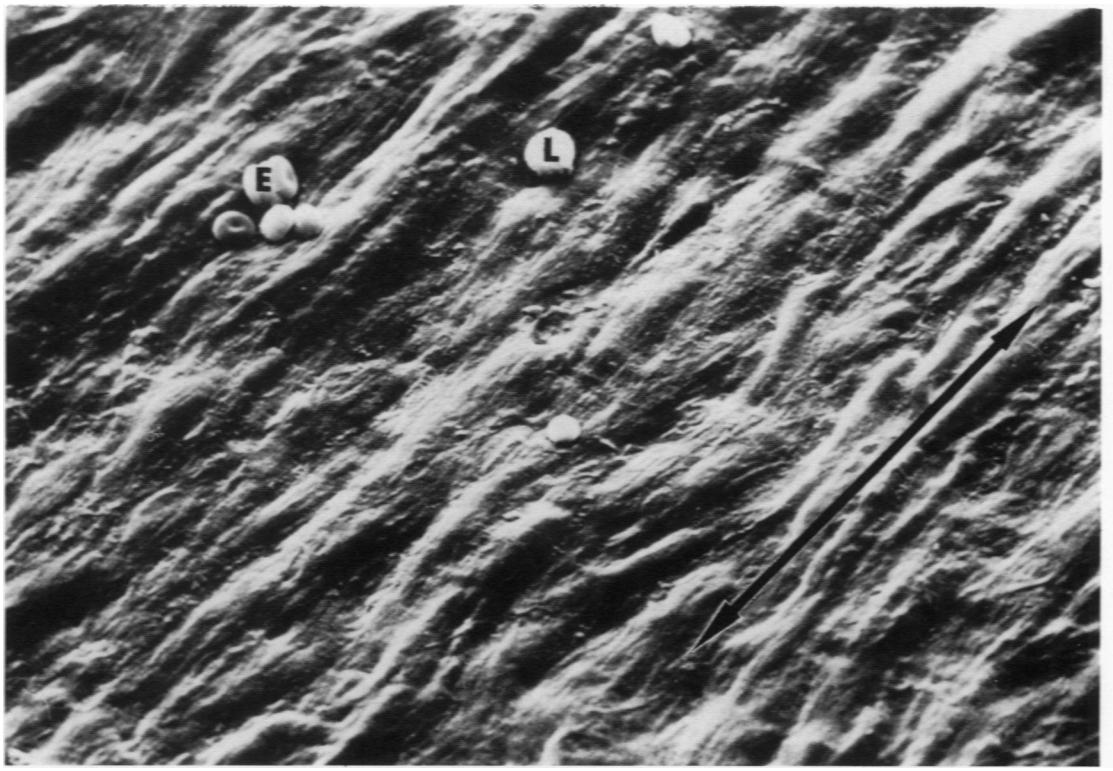

1

2

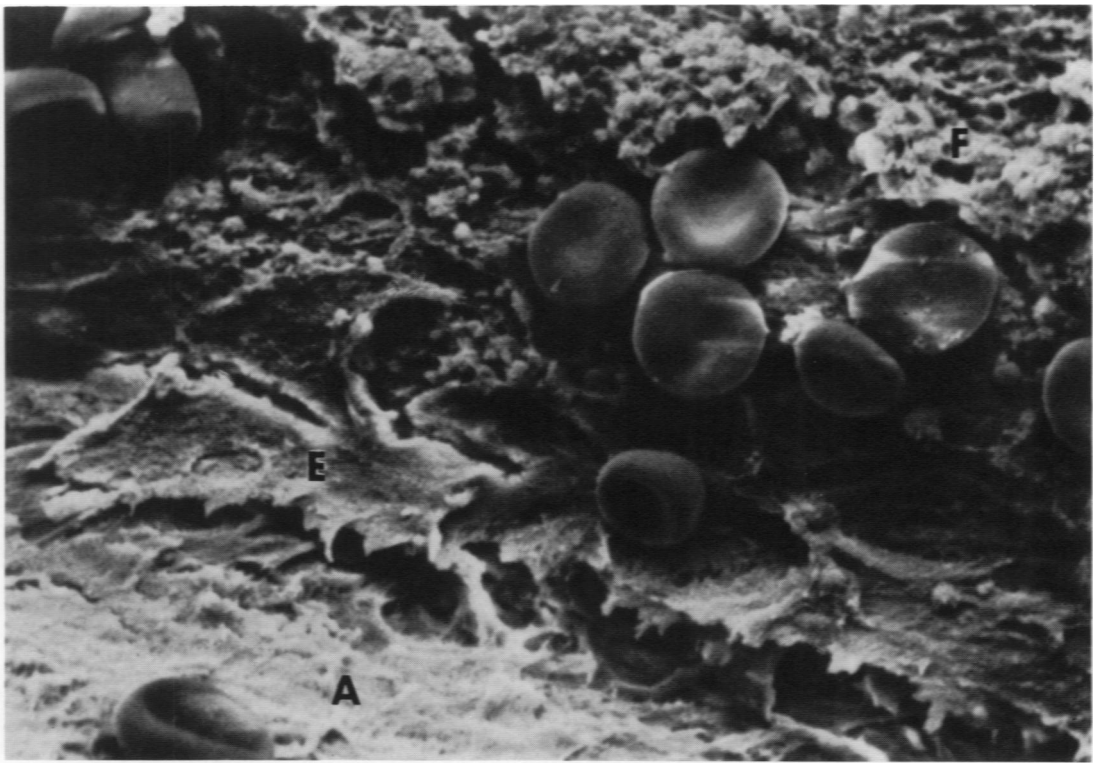

3

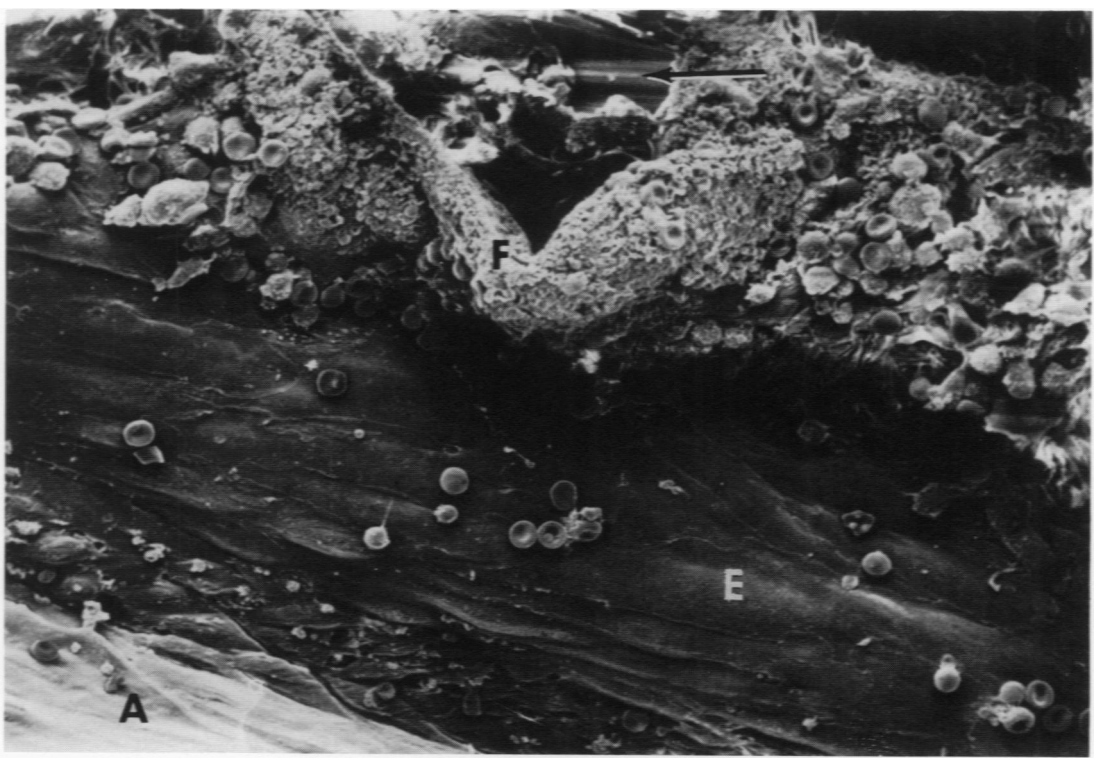

4

5

6

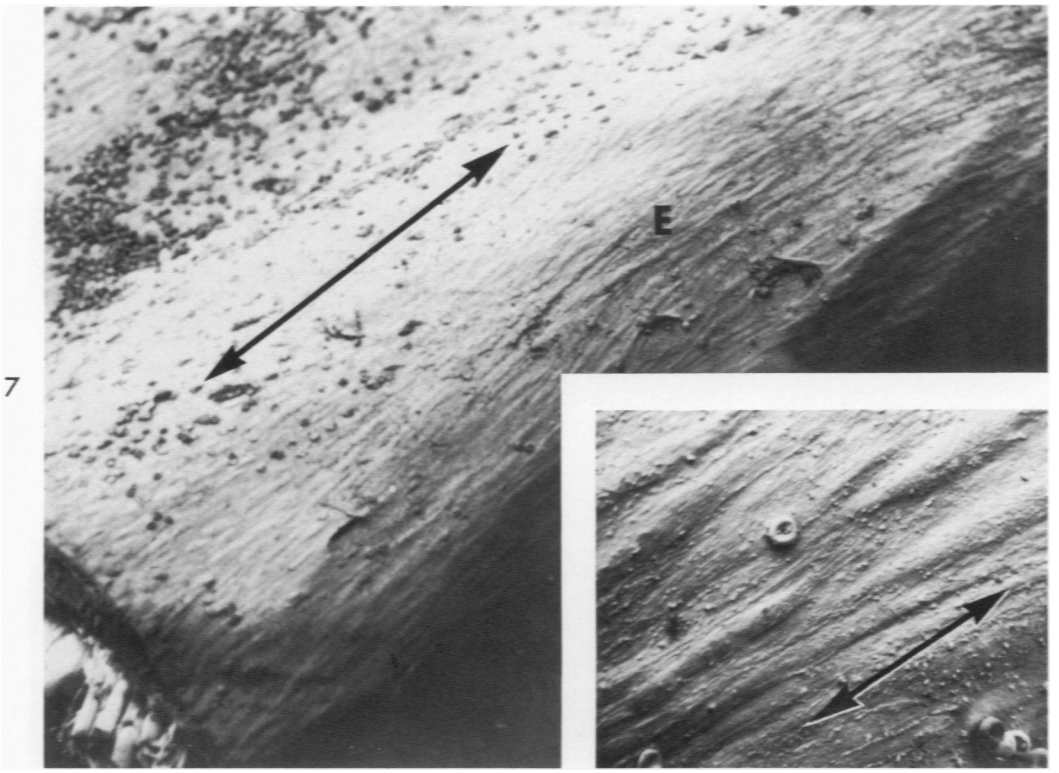

7

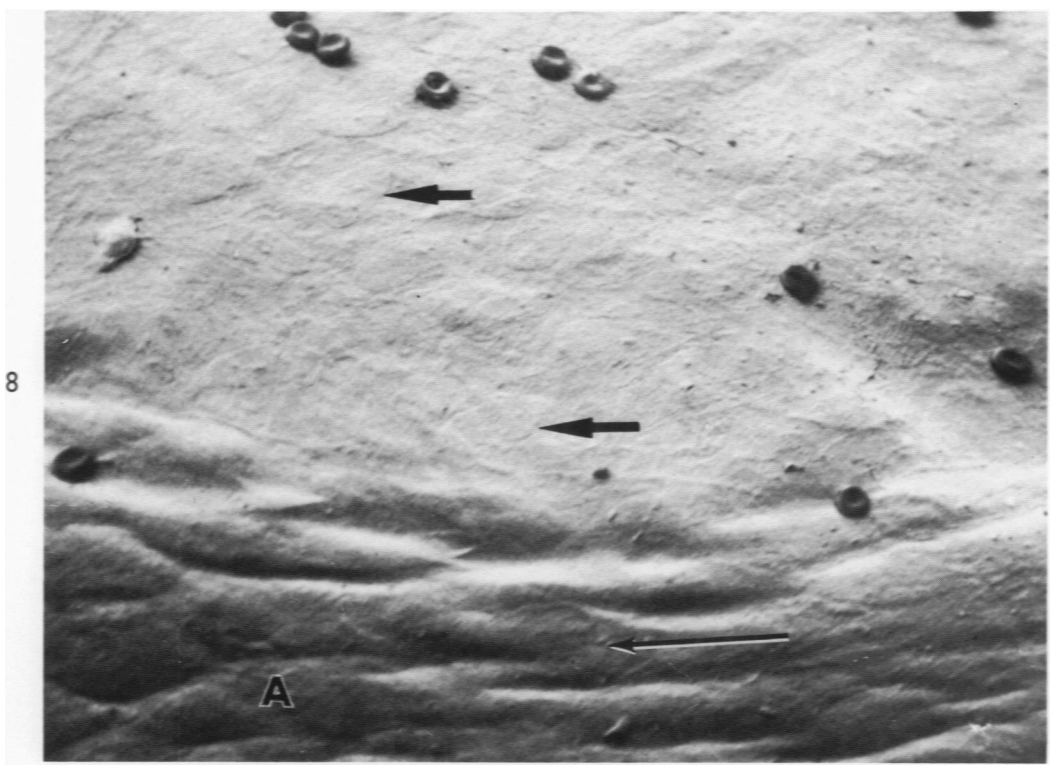

8

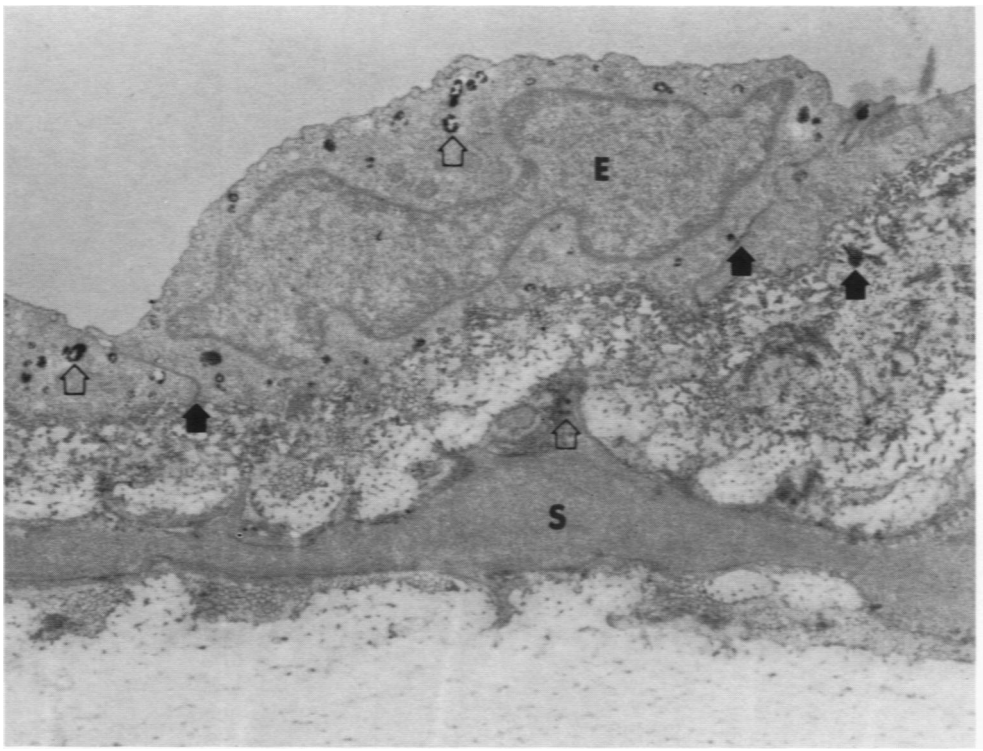

9

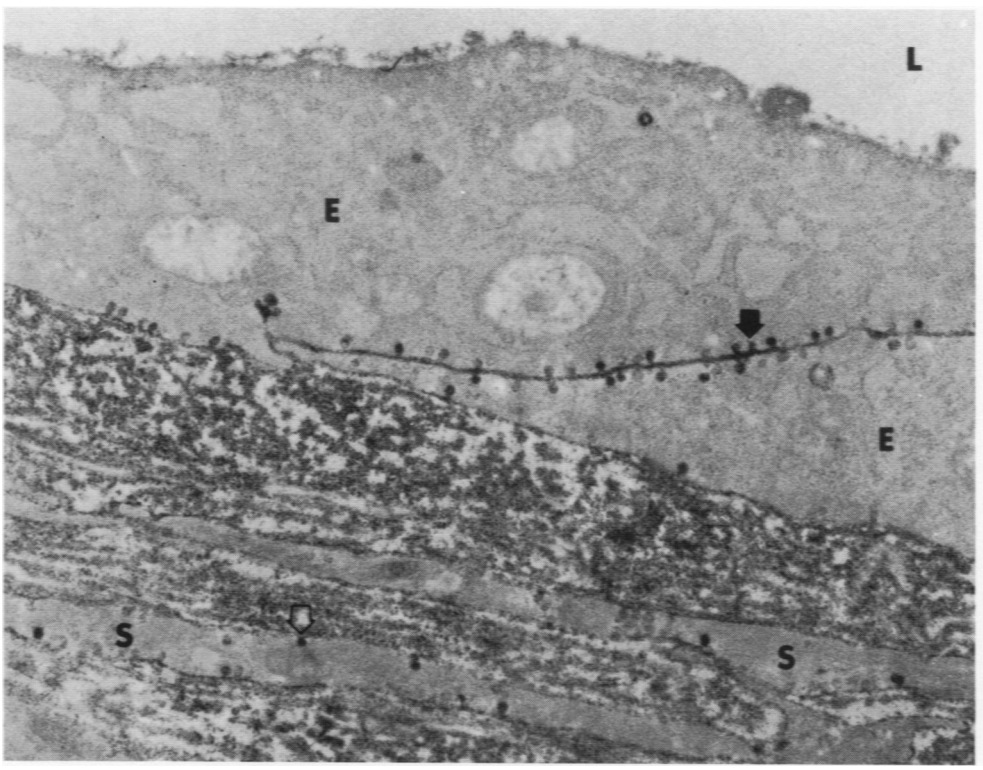

10

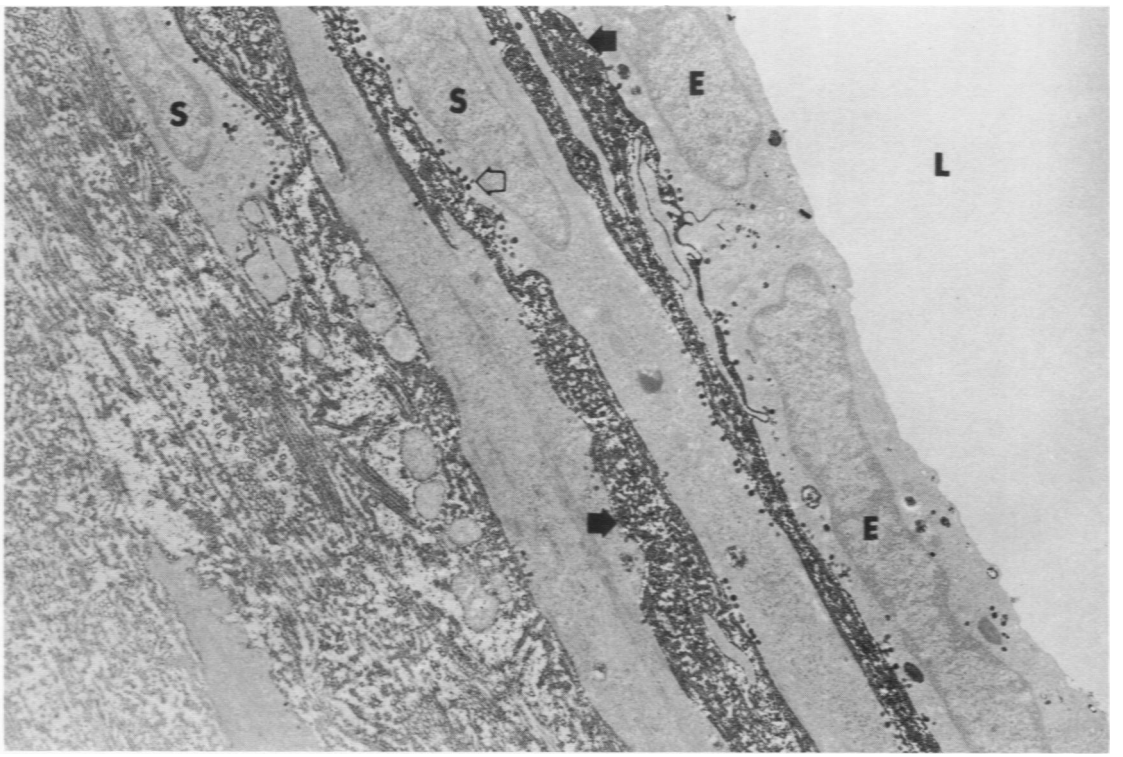

11

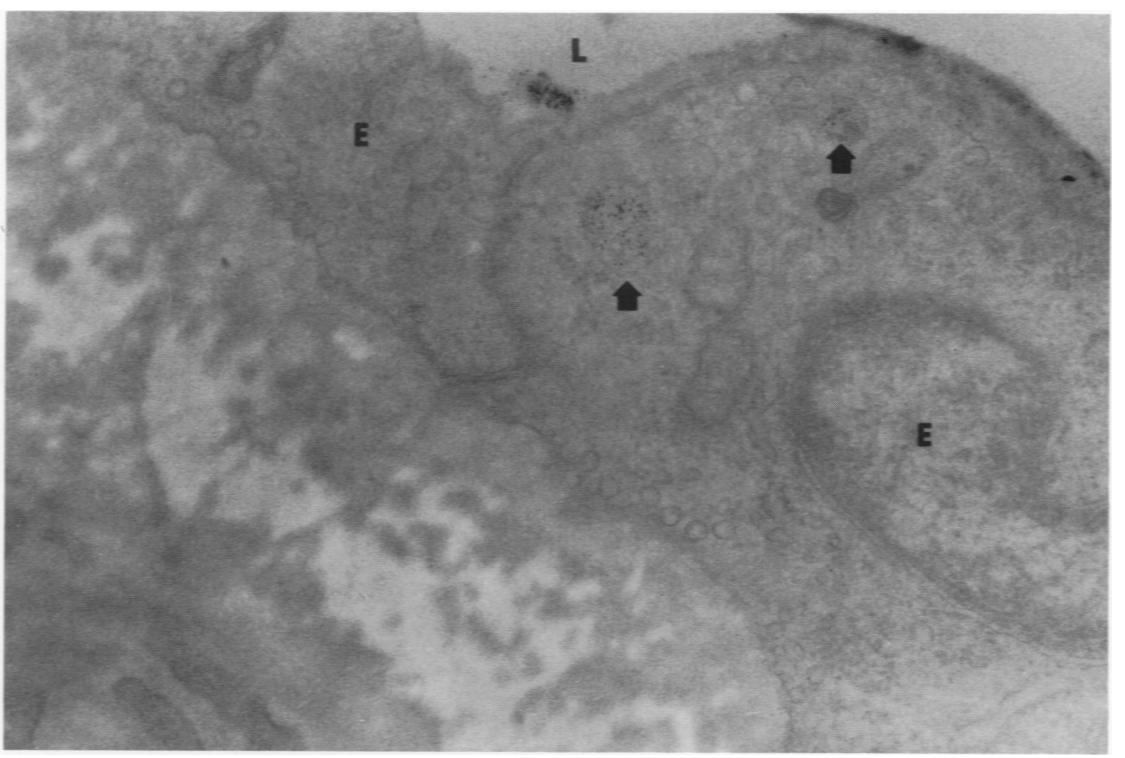

12

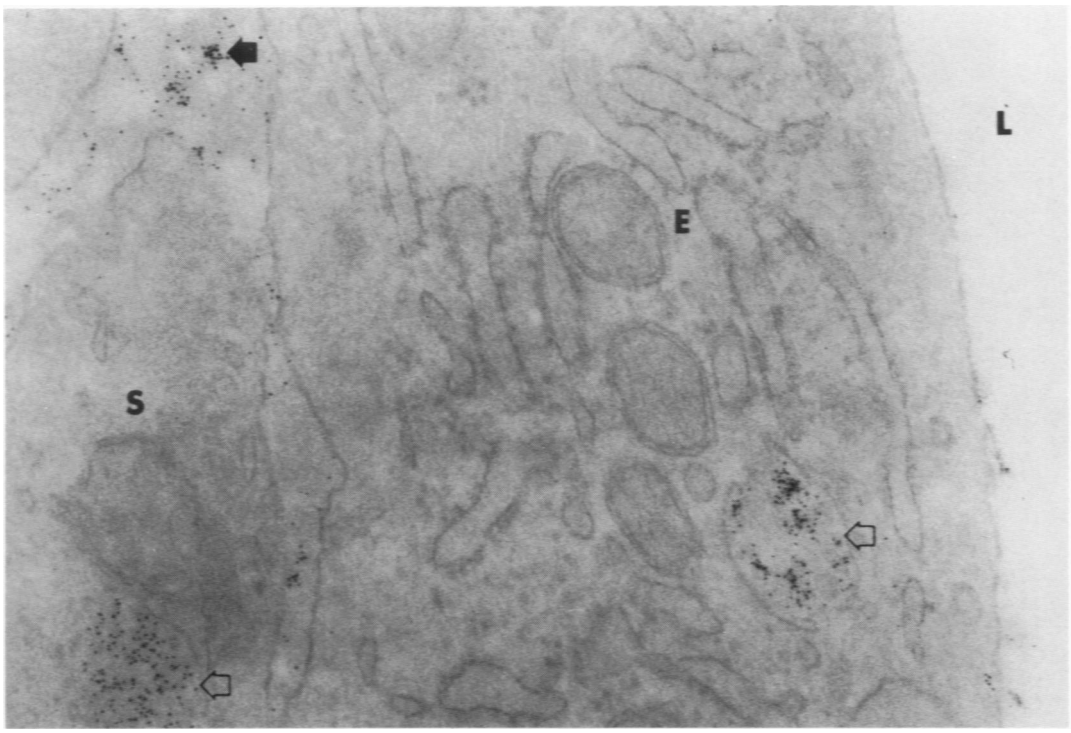

13

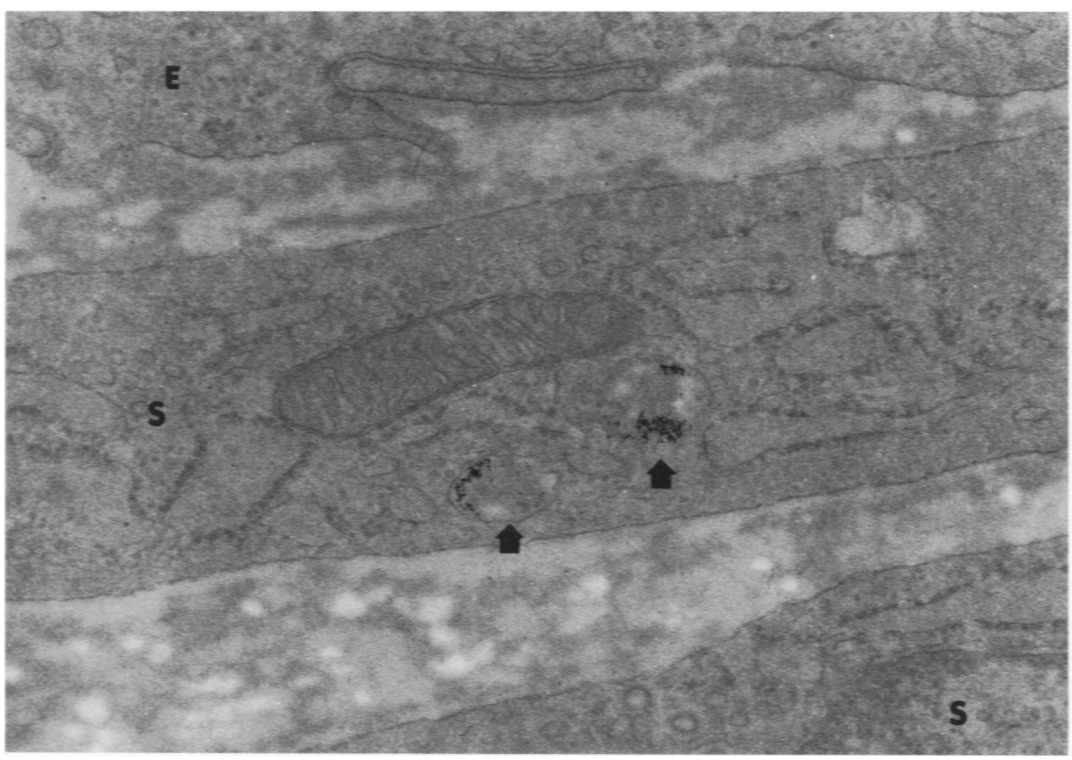

14

[*End of Article*]